Development of sigma-1 (σ_1) receptor fluorescent ligands as versatile tools to study σ_1 receptors☆

Carmen Abate[a,*], **Chiara Riganti**[b], **Maria Laura Pati**[a], **Dario Ghigo**[b], **Francesco Berardi**[a], **Timur Mavlyutov**[c], **Lian-Wang Guo**[c], and **Arnold Ruoho**[d]

[a]Dipartimento di Farmacia-Scienze Del Farmaco, Università Degli Studi di Bari ALDO MORO, Via Orabona 4, I-70125, Bari, Italy

[b]Department of Oncology, University of Turin, Via Santena 5/bis, 10126, Torino, Italy

[c]Department of Surgery, School of Medicine and Public Health, University of Wisconsin, Madison, USA

[d]Department of Neuroscience, School of Medicine and Public Health, University of Wisconsin, Madison, USA

Abstract

Despite their controversial physiology, sigma-1 (σ_1) receptors are intriguing targets for the development of therapeutic agents for central nervous system diseases. With the aim of providing versatile pharmacological tools to study σ_1 receptors, we developed three σ_1 fluorescent tracers by functionalizing three well characterized σ_1 ligands with a fluorescent tag. A good compromise between σ_1 binding affinity and fluorescent properties was reached, and the σ_1 specific targeting of the novel tracers was demonstrated by confocal microscopy and flow cytometry. These novel ligands were also successfully used in competition binding studies by flow cytometry, showing their utility in nonradioactive binding assays as an alternative strategy to the more classical radioligand binding assays. To the best of our knowledge these are the first σ_1 fluorescent ligands to be developed and successfully employed in living cells, representing promising tools to strengthen σ_1 receptors related studies.

Keywords

Sigma receptors; Fluorescent ligand

1. Introduction

The existence of sigma (σ) receptors was first reported in 1976 when they were considered as subtypes of opiate receptors [1]. Later studies clarified that they are a unique set of

---

proteins divided into two subtypes, namely σ_1 and σ_2 [2]. The σ_2 subtype is the lesser known: it has not yet been cloned, and different hypotheses about its identity have been formulated [3–5]. Despite this paucity of information, interest in σ_2 receptor research is on the increase because this subtype is overexpressed in several cancers and its activation through ligands leads cancer cells to death [6–9]. Worthy of note is also the efficacy of σ_2 ligands in resistant tumors that shed light on novel strategies for tumor treatments [10]. On the other hand, σ_1 receptor was cloned right after the two subtypes were discovered [11]. Several structures were proposed for this 223 amino-acids protein and the most accepted model represents the σ_1 receptor made of three hydrophobic regions two of which are trans-membrane spanning segments. The NH_2 and the COOH termini of the σ_1 protein are on the same side of the cell compartment where a possible endogenous ligand, not yet identified, regulates its function [12]. Progesterone, sphingolipid-derived amines (*D*-erythro-sphingosine) and more recently *N,N*-dimethyltryptamines have been proposed as σ_1 endogenous ligands [13–15]. Because of the important therapeutic potentials (e.g. treatment of anxiety, depression, schizophrenia, etc) linked to σ_1 receptor targeting, interest in σ_1 receptor research is on the increase [16]. Recent evidence has shown that σ_1 receptor can naturally form dimers and/or oligomer and that heteromers between σ_1 and D_2 receptor play an important role in cocaine addiction [17,18]. These dimers/oligomers may lead to different functional forms of the σ_1 receptor (such as agonist or antagonist activity). All these lines of evidence make novel pharmacological tools appealing for the study of the still controversial σ_1 receptor physiology. With this aim, we produced three σ_1 receptor fluorescent tracers starting from previously well characterized σ_1 receptor ligands. We adopted the same strategy that was shown to be successful for σ_2 fluorescent ligands: the appropriate σ_1 pharmacophore was linked through a spacer to a green emitting fluorescent tag [19–21]. In particular, as σ_1 pharmacophores we selected 4-methyl-1-[4-(6-methoxy-1,2,3,4-tetrahydronaphthalen-1-yl)butyl]piperidine PB190 and 4-methyl-1-[4-(6-methoxynaphthalen-1-yl)butyl]piperidine PB212 (Fig. 1) which were shown to be respectively a σ_1 selective agonist and a σ_1 selective antagonist by both *in vitro* and *in vivo* assays [22–26]. We also selected 4-cyclohexyl-1-[3-(5-methoxy-1,2,3,4-tetrahydronaphthalen-1-yl)propionyl]piperazine (Fig. 1) which showed excellent σ_1 affinity and σ_1 *vs* σ_2 selectivity [27]. The methoxy group present in these σ_1 ligands was replaced by a hexamethylenoxy chain carrying in the ω position a 4-*N,N*-dimethylphthalimide moiety. These choices were made on the basis of data obtained from σ_2 receptor fluorescent ligands: the position on the naphthalene or tetralin ring and the nature of the linker showed to be well tolerated with 4-*N,N*-dimethylphthalimide conferring optimal fluorescent properties that allowed successful experiments in living cells by flow cytometry and confocal microscopy.

2. Results and discussion

2.1. Chemistry

The synthetic pathway for final compounds **5, 6** and **9**, is depicted in Scheme 1. The already known piperidines PB190 and PB212 [22] and the piperazine **1** [27] were demethylated by reaction with BBr_3 to provide the corresponding phenolic intermediates **2, 3** and **8**, although phenol **3** was previously obtained through another synthetic pathway [28]. Alkylation of the phenolic intermediates **2, 3** and **8** with the already known mesyl derivative **4** [20] provided

final fluorescent compounds **5**, **6** and **9**. Final compounds **6** and **9** were converted into the corresponding hydrochloride salts with gaseous HCl, whereas **5** was converted into the corresponding oxalate salt.

2.2. σ Receptors radioligand binding

Results from binding assays are expressed as inhibition constants (K_i values) in Table 1. As in the σ_2 receptors fluorescent ligands, the introduction of the fluorescent tag connected through the hexamethylenoxy linker at the 2- or 5-position of the naphthalene and tetralin ring respectively, produced a decrease in the σ_1 receptor affinity with respect to the corresponding lead compounds. Only compound **5** presented affinity values at both σ receptors ($K_i = 3.61$ nM at the σ_1, and $K_i = 48.3$ nM at the σ_2) comparable to those of lead compound PB190 ($K_i = 1.01$ nM at the σ_1, and $K_i = 48.7$ nM at the σ_2). Final compounds **6** and **9** presented a 100-fold drop in the σ_1 affinity ($K_i = 5.20$ nM and $K_i = 13.1$ nM, respectively) in comparison to the lead compounds PB212 and **1**, respectively ($K_i = 0.03$ nM and $K_i = 0.11$ nM, respectively). By contrast, the affinity at the σ_2 receptors only slightly decreased for **6** (2.5-fold) in comparison to its lead compound PB212, whereas σ_2 receptor affinity of **9** was 5-fold higher than σ_2 receptor affinity displayed by **1**. Despite the decrease in the σ_1 affinity compared to the lead compounds, the three fluorescent ligands still demonstrated strong nanomolar σ_1 binding, and compounds **5** and **6** also kept a certain σ_1 *versus* σ_2 receptor selectivity (10-fold), which was lower (3-fold) in **9**. Taking these data together, the strategy adopted to obtain σ_2 receptor fluorescent ligands showed to be successful also for σ_1 receptor fluorescent ligands.

2.3. Fluorescent ligands studies

2.3.1. Fluorescent properties—The fluorescent properties are listed in Table 1. The three compounds displayed very similar maximum excitation wavelength (λex = 390 nm) and maximum emission wavelength (λem ~ 520 nm), with an important difference between λex and λem (i.e., Stokes shift) in accordance to the spectra recorded for the σ_2 ligands with the same fluorescent tag [20,21]. Measurement of quantum yields (QY) demonstrated the environment sensitive properties (low fluorescence intensity in polar solvent such as EtOH, but high fluorescence in nonpolar solvents such as CHCl$_3$), proper for the 4-*N,N*-dimethylphthalimide fluorescent tag, as recorded for σ_2 ligands.

2.3.2. Imaging of ARPE19 cells with compound 9 by confocal microscopy—In Fig. 2 the labeling of human retinal pigment epithelia ARPE19 cells with compound **9** shows fluorescent signals in intracellular membranes. The fluorescent signals were protected by PB190, indicating the specificity of binding to σ receptors. In these same cells, the cytoprotective properties of compound **9** were assessed by the 3-(4,5-dimethylthiazol-2-yl)-2,5-diphenyl-2H-tetrazolium bromide (MTT) viability assay upon toxicity mediated by paraquat (Fig. 1, in the supporting information), making clear that compound **9** protects against such toxicity and therefore may be useful for oxidative stress treatments.

2.3.3. Detection of σ_1 receptors by flow cytometry—Cellular uptake of compounds **5** and **6** was studied by flow cytometry in two human breast tumor MCF7 cell lines: MCF7wt and MCF7σ_1. Both these cell lines were thoroughly and previously characterized:

the former over expresses σ_2 receptors (B_{max} = 2.02 pmol/mg protein) [5,20] whereas σ_1 receptors' expression is very low (B_{max} = 0.17 pmol/mg protein) [5,29]; the latter is obtained by stable transfection of MCF7 cells with σ_1 c-DNA to obtain a good expression of σ_1 receptors (B_{max} = 3.45 pmol/mg protein) [21,29]. All of the experiments were performed by incubation of the two cell lines for 45 and 75 min with either compound **5** or **6** at 100 nM, as the fluorescence signal increased in a dose-dependent manner, reaching a plateau at 100 nM. Despite their 10-fold σ_1 *vs* σ_2 selectivity, compounds **5** and **6** still display σ_2 receptor affinity (K_i = 48.3 nM for **5** and K_i = 45.6 nM for **6**). Therefore, the σ_2 selective ligand 2-(3-(6,7-dimethoxy-3,4-dihydroisoquinolin-2(1*H*)-yl)propyl)-5-methoxy-3,4-dihydroisoquinolin-1(2*H*)-one **10** [30] (K_i = 2435 nM at the σ_1, and K_i = 4.24 nM at the σ_2) was used at 10 μM to mask the possible fluorescent signal generated by the σ_2 targeting of the fluorescent compounds. The σ_1 specificity of the fluorescent tracers (100 nM) was demonstrated by comparison of the fluorescent signals by MCF7σ_1 and MCF7wt, (Fig. 3) upon treatment with (+)-pentazocine and **10**. In MCF7wt cells, where the fluorescence intensity was very low in each experimental condition, no change in the fluorescent signal by either **5** or **6** was detected upon administration of (+)-pentazocine or **10** (Fig. 3, right panels). In MCF7σ_1 cells the administration of (+)-pentazocine (10 μM) strongly decreased the fluorescent signal by both **5** and **6** (with the signal by **5** completely abated) whereas, treatment with compound **10** (10 μM) only slightly decreased fluorescence by both the tracers. As, expected, co-administration of both (+)-pentazocine and **10** completely abated the fluorescent signals by both the tracers (Fig. 3, left panels). These results reflected the expression of σ_1 receptors in the MCF7 cell lines and suggested that these tracers, administered at 100 nM, bind σ_1 receptors rather specifically, with a negligible interference by σ_2 receptors. In MCF7σ_1, either **5** (100 nM) or **6** (100 nM) were dose dependently displaced (as demonstrated by the progressive decrease of fluorescence) by pre-incubation with increasing concentrations of either PB190 or PB212 (Figs. 4 and 5A and B; left panels; basal fluorescence of MCF7 cells in the presence of PB190 or PB212 reported in Fig. 2 in the supporting information), which were used as σ_1 reference non-fluorescent compounds (from 1 nM to 10 μM). The same experiment was performed with (+)-pentazocine and a dose-dependent displacement were again recorded, with more linear results obtained by 45 min incubation time (Fig. 6). By contrast, no differences were shown between the two incubation times studied (45 min or 75 min) when **5** or **6** were displaced by PB190 and PB212. As expected from a cell line with very low amount of σ_1 receptors, the displacement was far more modest in MCFwt (Figs. 4–6, A and B; right panels). The fluorescence intensity results obtained by either **5** or **6** in MCF7σ_1 cells by dose-dependent displacement of the σ_1 receptor ligands studied, served to generate binding curves for PB190, PB212 and (+)-pentazocine allowing the measurement of the IC_{50} values of these compounds for the human σ_1 receptors in MCF7 cells (Table 2). Differences between radioligand binding assays performed on animal tissues and human cells homogenates have already been reported for σ_1 receptors, with slightly lower binding affinities from the latter experiment [31]. The IC_{50} values obtained by flow cytometry on MCF7σ_1 cells were in accordance with such trend, demonstrating the utility of σ_1 receptors fluorescent ligand as tools to detect their presence in living cells and to conveniently perform σ_1 binding assays of novel ligands instead of the radioligand binding assays.

3. Conclusions

Three σ$_1$ fluorescent tracers were synthesized by functionalization of three well characterized σ$_1$ ligands with a fluorescent tag. A good compromise between binding affinity at the σ$_1$ subtype and fluorescent properties was obtained, with all the compounds displaying nanomolar σ$_1$ receptor affinity. Their σ$_1$ receptor specificities were demonstrated by protection with σ$_1$-specific compounds in different cell lines through different techniques: confocal microscopy (compound **9**) and flow cytometry (compounds **5** and **6**). We also demonstrated that through the use of these fluorescent tracers in flow cytometry, σ$_1$ binding assays of novel ligands can be conveniently performed in spite of the more classical radioligand binding assays that involves the use of radioligands such as [^{3}H]-(+)-pentazocine. To the best of our knowledge, these compounds are the first σ$_1$ fluorescent ligands to be produced and successfully employed, and they emerge as useful tools to empower σ$_1$ receptors studies.

4. Experimental section

4.1. Chemistry

Both column chromatography and flash column chromatography were performed with 60 Å pore size silica gel as the stationary 300 phase (1:30 w/w, 63–200 μm particle size, from ICN and 1:15 w/w, 15–40 μm particle size, from Merck, respectively). Melting points were determined in open capillaries on a Gallenkamp electrothermal apparatus. Purity of tested compounds was established by combustion analysis, confirming a purity >95%. Elemental analyses (C, H, N) were performed on an Eurovector Euro EA 3,000 analyzer; the analytical results were within ±0.4% of the theoretical values, unless otherwise indicated.^{1}H NMR spectra were recorded on a Mercury Varian 300 MHz using CDCl$_3$ as solvent, unless otherwise reported. The following data were reported: chemical shift (δ) in ppm, multiplicity (s, singlet; d, doublet; t, triplet; q, quadruplet; m, multiplet), integration and coupling constants in hertz. Recording of mass spectra was done on an Agilent 6890-5973 MSD gas chromatograph/mass spectrometer and on an Agilent 1100 series LC–MSD trap system VL mass spectrometer; only significant *m/z* peaks, with their percentages are reported in parentheses. Chemicals were from Aldrich, TCI and Alfa Aesar and were used without any further purification.

4.2. General procedure for the synthesis of phenolic intermediates (2, 3, 8)

A solution of one among the methoxy derivatives PB190, PB212 and **1** (1.0 mmol) in anhydrous CH$_2$Cl$_2$ (10 mL) and under Argon was cooled to −78 °C and then added in a dropwise manner with BBr$_3$ (3.0 mmol, 0.3 mL). The mixture was stirred overnight under argon while it slowly reached room temperature. After cooling in an ice bath, H$_2$O was added to the mixture which was basified with Na$_2$CO$_3$. The resulting mixture was extracted with CH$_2$Cl$_2$ (3 × 10 mL) and the organic phases collected, dried (Na$_2$SO$_4$) and concentrated under reduced pressure to afford crude oils which provided the title compounds upon purification through column chromatography (CH$_2$Cl$_2$/MeOH, 95:5).

4.2.1. 5-[4-(4-Methylpiperidine-1-yl)butyl]-5,6,7,8-tetrahydronaphthalen-2-ol (2)

—was obtained in 69% yield (0.204 g) as beige solid: mp = 184–186 °C; GC–MS *m/z*: 301 (M[+], 20), 112 (100); LC-MS (ESI[−]) *m/z*: 300 [M−H][−].

4.2.2. 5-[4-(4-Methylpiperidine-1-yl)butyl]naphthalen-2-ol (3)—was obtained in

69% yield (0.202 g) as beige solid: mp = 182–184 °C (literature [28] mp = 183–185 °C); GC–MS *m/z*: 297 (M[+], 20), 112 (100); LC-MS (ESI[−]) *m/z*: 296 [M−H][−]; LC-MS-MS 296: 156.

4.2.3. 4-Cyclohexyl-1-[3-(5-hydroxy-1,2,3,4-tetrahydronaphthalen-1-yl)propionyl]piperazine (8)—was obtained in 90% yield (0.33 g) as sticky solid.[1]H

NMR δ 1.05–1.35 [m, 6H, cyclohexyl], 1.55–2.05 (m, 10H, COCH$_2$C*H*$_2$CHC*H*$_2$C*H*$_2$ and cyclohexyl CH$_2$), 2.20–2.45 (m, 3H, benzyl CH and CH$_2$), 2.50–2.58 (m, 4H, CH$_2$ piperazine), 2.60–2.75 (m, 2H, CH$_2$CO), 2.80–2.85 (m, 1H, CHN), 4.38–4.70 [m, 4H, CON(CH$_2$)$_2$], 5.20 (broad s, 1H, OH), 6.60 (d, *J* = 7.15 Hz, 1H aromatic), 6.78 (d, *J* = 7.7 Hz, 1H, aromatic), 7.00 (t, *J* = 7.8 Hz, 1H, aromatic); GC–MS *m/z*: 370 (M[+], 30), 138 (70), 125 (100), 112 (80).

4.3. General procedure for the synthesis of final fluorescent compounds (5, 6 and 9)

A solution in DMF (10 mL) of one among the phenol intermediates **2** or **3** or **8** (1.0 mmol) was added with the mesyl derivative **4** (1.0 mmol, 0.37 g) and K$_2$CO$_3$ (1.2 mmol, 0.16 g) to provide a mixture which was stirred at 150 °C overnight. After concentration under reduced pressure the crude residue which was taken up with water was extracted with CH$_2$Cl$_2$ (3 × 10 mL) and the organic phases collected were dried (Na$_2$SO$_4$) and evaporated under reduced pressure to provide a crude oil which was purified by column chromatography (CH$_2$Cl$_2$/ MeOH, 95:5) to afford the title compounds.

4.3.1. 5-(Dimethylamino)-2-(6-((5-(4-(4-methylpiperidin-1-yl) butyl)-5,6,7,8-tetrahydronaphthalen-2-yl)oxy)hexyl)isoindoline-1,3-dione (5)—The title

compound was obtained in a 50% yield (0.286 g) as a bright yellow oil.^{1}H NMR δ 0.98 (d, *J* = 5.7 Hz, 3H, CHC*H*$_3$), 1.25–2.00 [m, 19H, N(CH$_2$)$_2$, CH$_2$(C*H*$_2$)$_4$, CH(C*H*$_2$)$_3$ e NH], 2.25–2.40 (m, 3H, benzyl CH and CH$_2$), 2.60–2.70 (m, 4H, N(CH*H*)$_2$ and CH$_2$CH$_2$C*H*$_2$N), 2.85–2.95 (m, 2H, N(CH*H*)$_2$), 3.10 [s, 6H, N(CH$_3$)$_2$], 3.62 (t, *J* = 7.15 Hz, 2H, (CO)$_2$NCH$_2$), 3.88 (t, *J* = 6.6 Hz, 2H, OCH$_2$), 6.50–7.65 (m, 6H, aromatic); LC–MS (ESI[+]) *m/z*: 574 [M+H][+]; LC–MS–MS 574: 203. Anal. (C$_{36}$H$_{51}$N$_3$O$_3$·C$_2$O$_4$H$_2$·½H$_2$O) C, H, N.

4.3.2. 5-(Dimethylamino)-2-{6-[(5-(4-(4-methylpiperidin-1-yl) butyl)naphthalen-2-yl)oxy]hexyl}isoindole-1,3-dione (6)—The title compound was

obtained in a 50% yield (0.284 g) as a bright yellow oil.^{1}H NMR δ 0.95–1.00 (m, 3H, NHCH$_3$), 1.15–2.05 [m, 17H, CH(CH$_2$)$_2$, (CO)$_2$NCH$_2$(C*H*$_2$)$_4$CH$_2$ and ArCH$_2$(C*H*$_2$)$_2$], 2.60–2.75 [m, 2H, N(CH*H*)$_2$], 2.85–2.95 [m, 2H, N(CH*H*)$_2$], 2.98–3.05 [m, 4H, Ar(CH$_2$)$_3$C*H*$_2$N], 3.10 [s, 6H, N(CH$_3$)$_2$], 3.65 (t, *J* = 7.15 Hz, 2H, (CO)$_2$NCH$_2$), 4.05 (t, *J* = 6.6 Hz, 2H, OCH$_2$), 6.70–8.05 (m, 9H, aromatic); LC–MS (ESI[+]) *m/z*: 570 [M+H][+]; LC–MS–MS 570: 203. Anal. (C$_{36}$H$_{47}$N$_3$O$_3$·HCl·1.75H$_2$O) C, H, N.

4.3.3. 2-(6-((5-(3-(4-Cyclohexylpiperazin-1-yl)-3-oxopropyl)-5,6,7,8-tetrahydronaphthalen-1-yl)oxy)hexyl)-5-(dimethylamino) isoindole-1,3-dione

(8)—The title compound was obtained in a 57% yield as a yellow oil (0.366 g).^{1}H NMR δ 1.05–2.05 [m, 24H, piperazine CH_2, $OCH_2(CH_2)_4$, $CH(CH_2)_3$], 2.20–2.85 [m, 10H, $CHN(CH_2)_2$, CH_2CO, benzyl CH and CH_2], 3.11 [s, 6H, $(NCH_3)_2$], 3.38–3.42 [m, 2H, $CON(CHH)_2$], 3.58-3.45 [m, 4H, $(CO)_2NCH_2$ and $CON(CHH)_2$], 3.90 (t, 2H, $J = 6.1$ Hz, OCH_2), 6.60–6.65 (m, 6H, aromatic); LC–MS (ESI$^+$) m/z: 665 [M+Na]$^+$; LC–MS–MS 665: 497, 393. Anal. ($C_{39}H_{54}N_4O_4$·2HCl) C, H, N.

4.4. Biology

4.4.1. Materials

—(+)-Pentazocine was purchased from Sigma–Aldrich (Milan, Italy), and 1,3-di-2-tolylguanidine (DTG) from Tocris Cookson Ltd., U.K. [^{3}H]-DTG (50 Ci/mmol), and (+)-[^{3}H]-pentazocine (30 Ci/mmol) were purchased from PerkinElmer Life and Analytical Sciences (Boston, MA). Male Dunkin guinea pigs and Wistar Hannover rats (250–300 g) were from Harlan, Italy. Cell culture reagents were purchased from EuroClone (Milan, Italy).

4.4.2. Competition binding assays

—All the procedures for the binding assays were previously described. σ$_1$ And σ$_2$ receptor binding were carried out according to Berardi et al. [27]. [^{3}H]-DTG, 1,3-di-2-tolylguanidine (30 Ci/mmol) and (+)-[^{3}H]-pentazocine (34 Ci/mmol) were purchased from PerkinElmer Life Sciences (Zavantem, Belgium). DTG was purchased from Tocris Cookson Ltd. (UK). (+)-Pentazocine was obtained from Sigma–Aldrich-RBI s.r.l. (Milan, Italy). Male Dunkin guinea pigs and Wistar Hannover rats (250–300 g) were from Harlan (Italy). The specific radioligands and tissue sources were, respectively: (a) σ$_1$ receptor, (+)-[^{3}H]-pentazocine, guinea pig brain membranes without cerebellum; (b) σ$_2$ receptor, [^{3}H]-DTG in the presence of 1 μm (+)-pentazocine to mask σ$_1$ receptors, rat liver membranes. The following compounds were used to define the specific binding reported in parentheses: (a) (+)-pentazocine (73–87%), (b) DTG (85–96%). Concentrations required to inhibit 50% of radioligand specific binding (IC50) were determined using six to nine different concentrations of the drug studied in two or three experiments with samples in duplicate. Scatchard parameters (K_d and B_{max}) and apparent inhibition constants (Ki values) were determined by nonlinear curve fitting, using Prism GraphPad software (version 3.0) [32].

4.4.3. Cell culture

—Human breast adenocarcinoma cell line (MCF7) was purchased from ICLC (Genoa, Italy), and were stably transfected with σ$_1$-receptor c-DNA (MCF7σ$_1$) as already described [29]. Cells were grown in DMEM high-glucose medium supplemented with fetal bovine serum (10%), and penicillin-streptomycin (1%) in a humidified incubator at 37 °C with a CO_2 atmosphere. Human retinal pigment epithelia ARPE19 cells were purchased from ATCC and grown in complete growth medium (DMEM supplemented with fetal bovine serum 10%) and penicillin-streptomycin (1%) in cell culture incubator with 5% CO_2.

4.4.4. ARPE19 cell imaging

—Drug treatment and imaging of ARPE cells was done in HBSS. For control, some wells were pretreated with 100 μMPB190 for 40 min. Cells were

further treated with compound **9** 0.5 μMfor 40 min, then rinsed twice in HBSS and imaged upon excitation wavelength of 408 nm and emission detection of 525 nm under a Nikon A1R laser confocal microscope (Nikon, Tokyo, Japan) supplied with green 488 nm Argon laser, red 561 nm DPSS laser through a Apo60X VC oil-immersion objective with NIS elements software.

4.4.5. MTT cell viability assay—ARPE19 cells were seeded to 96 well plates to a density of 30,000 cells/well and grown in complete growth medium to reach 100% confluency. Then 1 mM toxin Paraquat was applied with or without various concentrations of compound **9** and cells were incubated for 24 h in complete growth media. Then wells were quickly aspirated and MTT (Sigma–Aldrich M2128) was applied under the dim light at concentration 0.5 mg/mL in phenol red free DMEM (100 μL/well) supplemented with fetal bovine serum 0.5%. After 3 h of incubation 100 μL of 10% Sodium Dodecyl Sulfate (SDS) was added per each well. Plates were left overnight in cell culture incubator to dissolve precipitate. Absorbance at $\lambda = 540$ nm was detected in 96 well plate reader.

4.4.6. Flow cytometry studies—MCF7 and MCF7σ_1 cells were incubated with increasing concentrations (0.1,1,10, and 100 nmol/L and 1 and 10 μmol/L) of either PB190 or PB212 followed by 100 nmol/L of either compounds **5** or **6** for 45 or 75 min at 37 °C. To mask σ_2 receptors, compound **10** (10 μmol/L) was co-incubated. When indicated, cells were treated with increasing concentrations (1, 10, and 100 nmol/L and 1 and 10 μmol/L) of (+)-pentazocine or PB190 or PB212, followed by 100 nmol/L of compounds **5** or **6** for 45 or 75 min at 37 °C. At the end of the incubation periods, cells were washed twice with PBS, detached with 200 μL of Cell Dissociation Solution (Sigma Chemical Co.) for 10 min at 37 °C, centrifuged at 13,000 g for 5 min and resuspended in 500 μL of PBS. The fluorescence was recorded using a Bio-Guava® easyCyte™ 5 Flow Cytometry System (Millipore, Billerica, MA), with a 530 nm band pass filter. For each analysis, 50,000 events were collected and analyzed with the InCyte software (Millipore).

4.5. Fluorescence spectroscopy

Emission and excitation spectra of compounds **5, 6** and **9**, were determined in CHCl$_3$ and in PBS buffer solution as previously reported. Fluorescence quantum yields were calculated with respect to quinine sulfate as previously reported [19].

Supplementary Material

Refer to Web version on PubMed Central for supplementary material.

Abbreviations

DTG	1,3-di-2-tolylguanidine
DMEM	Dulbecco's modified Eagle's medium
PBS	Phosphate buffered saline
SDS	Sodium dodecyl sulfate

References

1. Martin WR, Eades CG, Thompson JA, Huppler RE, Gilbert PE. The effect of morphine- and nalorphine-like drugs in the nondependent and morphine-dependent chronic spinal dog. J. Pharmacol. Exp. Ther. 1976; 197:517–532. [PubMed: 945347]

2. Quirion R, Bowen WD, Itzhak Y, Junien JL, Musacchio JM, Rothman RB, Su TP, Tam SW, Taylor DP. A proposal for the classification of sigma binding sites. Trends Pharmacol. Sci. 1992; 13:85–86. [PubMed: 1315463]

3. Colabufo NA, Berardi F, Abate C, Contino M, Niso M, Perrone R. Is the σ_2 receptor a histone binding protein? J. Med. Chem. 2006; 49:4153–4158. [PubMed: 16821775]

4. Xu J, Zeng C, Chu W, Pan F, Rothfuss JM, Zhang F, Tu Z, Zhou D, Zeng D, Vangveravong S, Johnston F, Spitzer D, Chang KC, Hotchkiss RS, Hawkins WG, Wheeler KT, Mach RH. Identification of the PGRMC1 protein complex as the putative sigma-2 receptor binding site. Nat. Commun. 2011; 2:380. [PubMed: 21730960]

5. Abate C, Niso M, Infantino V, Menga A, Berardi F. Elements in support of the 'non-identity' of the PGRMC1 protein with the σ_2 receptor. Eur. J. Pharmacol. 2015; 758:16–23. [PubMed: 25843410]

6. Zeng C, Rothfuss J, Zhang J, Chu W, Vangveravong S, Tu Z, Pan F, Chang KC, Hotchkiss R, Mach RH. Sigma-2 ligands induce tumour cell death by multiple signalling pathways. Br. J. Cancer. 2012; 106:693–701. [PubMed: 22251921]

7. Hornick JR, Vangveravong S, Spitzer D, Abate C, Berardi F, Goedegebuure P, Mach RH, Hawkins WG. Lysosomal membrane permeabilization is an early event in sigma-2 receptor ligand mediated cell death in pancreatic cancer. J. Exp. Clin. Cancer Res. 2012; 31:41. [PubMed: 22551149]

8. Abate C, Perrone R, Berardi F. Classes of sigma$_2$ (σ_2) receptor ligands: structure affinity relationship (SAfiR) studies and antiproliferative activity. Curr. Pharm. Des. 2012; 18:938–949. [PubMed: 22288411]

9. Abate C, Niso M, Contino M, Colabufo NA, Ferorelli S, Perrone R, Berardi F. 1-Cyclohexyl-4-(4-arylcyclohexyl)piperazines: mixed σ and human $_{8-}$ $_7$ sterol isomerase ligands with antiproliferative and P-glycoprotein inhibitory activity. Chem. Med. Chem. 2011; 6:73–80. [PubMed: 21069657]

10. Niso M, Abate C, Contino M, Ferorelli S, Azzariti A, Perrone R, Colabufo NA, Berardi F. Sigma-2 receptor agonists as possible antitumor agents in resistant tumors: hints for collateral sensitivity. Chem. Med. Chem. 2013; 8:2026–2035. [PubMed: 24106081]

11. Hanner M, Moebius FF, Flandorfer A, Knaus HG, Striessnig J, Kempner E, Glossmann H. Purification, molecular cloning, and expression of the mammalian sigma1-binding site. Proc. Natl. Acad. Sci. U. S. A. 1996; 93:8072–8077. [PubMed: 8755605]

12. Pal A, Chu UB, Ramachandran S, Grawoig D, Guo LW, Hajipour AR, Ruoho AE. Juxtaposition of the steroid binding domain-like I and II regions constitutes a ligand binding site in the σ_1 receptor. J. Biol. Chem. 2008; 283:19646–19656. [PubMed: 18467334]

13. Johannessen M, Fontanilla D, Mavlyutov T, Ruoho AE, Jackson MB. Antagonist action of progesterone at σ-receptors in the modulation of voltage-gated sodium channels. Am. J. Physiol. Cell Physiol. 2011; 300:328–337.

14. Ruoho AE, Chu UB, Ramachandran S, Fontanilla D, Mavlyutov T, Hajipour AR. The ligand binding region of the sigma-1 receptor: studies utilizing photoaffinity probes, sphingosine and N-alkylamines. Curr. Pharm. Des. 2012; 18:920–929. [PubMed: 22288412]

15. Fontanilla D, Johannessen M, Hajipour AR, Cozzi NV, Jackson MB, Ruoho AE. The hallucinogen N,N-dimethyltryptamine (DMT) is an endogenous sigma-1 receptor regulator. Science. 2009; 323:934–937. [PubMed: 19213917]

16. Banister SD, Kassious M. The therapeutic potential of sigma (σ) receptor for the treatment of central nervous system diseases: evaluation of the evidence. Curr. Pharm. Des. 2012; 18:884–901. [PubMed: 22288410]

17. Chu UB, Ramachandran S, Hajipour AR, Ruoho AE. Photoaffinity labeling of the sigma-1 receptor with *N*-[3-(4-nitrophenyl)propyl]-*N*-dodecylamine: evidence of receptor dimers. Biochemistry. 2013; 52:859–868. [PubMed: 23324054]

18. Navarro G, Moreno E, Bonaventura J, Brugarolas M, Farré D, Aguinaga D, Mallol J, Cortés A, Casado V, Lluis C, Ferre S, Franco R, Canela E, McCormick PJ. Cocaine inhibits dopamine D_2 receptor signaling via sigma-1-D_2 receptor heteromers. PLoS One. 2013; 8:61245.

19. Abate C, Hornick JR, Spitzer D, Hawkins WJ, Niso M, Perrone R, Berardi F. Fluorescent derivatives of σ receptor ligand 1-cyclohexyl-4-[3-(5-methoxy-1,2,3,4-tetrahydronaphthalen-1-yl)-propyl]piperazine (PB28) as a tool for uptake and cellular localization studies in pancreatic tumor cells. J. Med. Chem. 2011; 54:5858–5867. [PubMed: 21744858]

20. Abate C, Niso M, Marottoli R, Riganti C, Ghigo D, Ferorelli S, Ossato G, Perrone R, Lacivita E, Lamb DC, Berardi F. Novel derivatives of 1-cyclohexyl-4-[3-(5-methoxy-1,2,3,4-tetrahydronaphthalen-1-yl)propyl]piperazine (PB28) with improved fluorescent and σ receptors binding properties. J. Med. Chem. 2014; 57:3314–3323. [PubMed: 24697311]

21. Niso M, Riganti C, Pati ML, Ghigo D, Berardi F, Abate C. Novel and selective fluorescent σ_2-receptor ligand with a 3,4-dihydroisoquinolin-1-one scaffold: a tool to study σ_2 receptors in living cells. Chem. Bio. Chem. 2015; 16:1078–1083.

22. Berardi F, Ferorelli S, Abate C, Pedone MP, Colabufo NA, Contino M, Perrone R. Methyl substitution on the piperidine ring of *N*-[ω-(6-methoxynaphthalen-1-yl)alkyl] derivatives as a probe for selective binding and activity at the σ_1 receptor. J. Med. Chem. 2005; 48:8237–8244. [PubMed: 16366605]

23. Gasparre G, Abate C, Berardi F, Cassano G. The sigma-1 receptor antagonist PB212 reduces the Ca^{2+}-release through the inositol (1,4,5)-trisphosphate receptor in SK-N-SH cells. Eur. J. Pharmacol. 2012; 684:59–63. [PubMed: 22465185]

24. Skuza G, Szymanska M, Budziszewska B, Abate C, Berardi F. Effects of PB190 and PB212, new σ receptor ligands, on glucocorticoid receptor-mediated genetranscription in LMCAT cells. Pharmacol. Rep. 2011; 63:1564–1568. [PubMed: 22358106]

25. Skuza G, Sadaj W, Kabzinski M, Cassano G, Gasparre G, Abate C. The effects of new sigma (σ) receptor ligands, PB190 and PB212, in the models predictive of antidepressant activity. Pharmacol. Rep. 2014; 66:320–324. [PubMed: 24911087]

26. Moritz C, Berardi F, Abate C, Peri F. Live imaging reveals a new role for the sigma-1 (σ_1) receptor in allowing microglia to leave brain injuries. Neurosci. Lett. 2015; 591:13–18. [PubMed: 25666889]

27. Berardi F, Abate C, Ferorelli S, Uricchio V, Colabufo NA, Niso M, Perrone R. Exploring the importance of piperazine N-atoms for σ_2 receptor affinity and activity in a series of analogs of 1-cyclohexyl-4-[3-(5-methoxy-1,2,3,4-tetrahydronaphthalen-1-yl)propyl]piperazine (PB28). J. Med. Chem. 2009; 52:7817–7828. [PubMed: 19842660]

28. Gao M, Wang M, Hutchins GD, Zheng QH. Synthesis of carbon-11-labeled piperidine ring of *N*-[ω-(6-methoxynaphthalen-1-yl)alkyl] derivatives as new selective PET σ_1 receptor probes. Appl. Radiat. Isot. 2010; 68:459–465. [PubMed: 20060731]

29. Abate C, Ferorelli S, Niso M, Lovicario C, Infantino V, Convertini P, Perrone R, Berardi F. 2-Aminopyridine derivatives as potential σ_2 receptor antagonists. Chem. Med. Chem. 2012; 7:1847–1857. [PubMed: 22890883]

30. Abate C, Selivanova SV, Müller A, Krämer SD, Schibli R, Marottoli R, Perrone R, Berardi F, Niso M, Ametamey SM. Development of 3,4-dihydroisoquinolin-1(2*H*)-one derivatives for the Positron Emission Tomography (PET) imaging of σ_2 receptors. Eur. J. Med. Chem. 2013; 69:920–930. [PubMed: 24161678]

31. Berardi F, Abate C, Ferorelli S, Colabufo NA, Perrone R. 1-Cyclohexylpiperazine and 3,3-dimethylpiperidine derivatives as sigma-1 (σ_1) and sigma-2 (σ_2) receptor ligands: a review. Cent. Nerv. Syst. Agents Med. Chem. 2009; 9:205–219. [PubMed: 20021355]

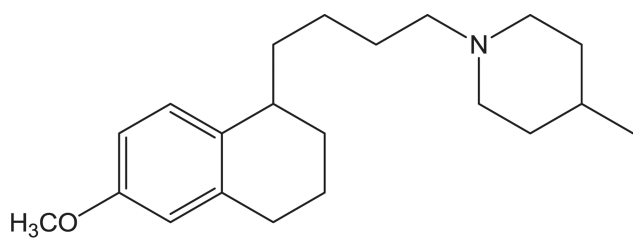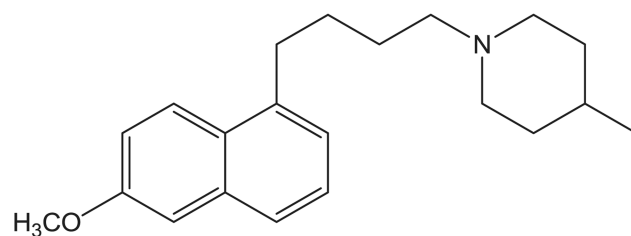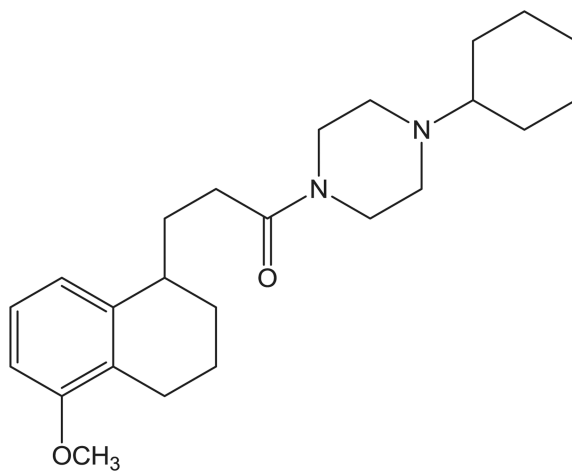32. Prism Software, Version 3.0 for Windows. San Diego, CA: GraphPad Software, Inc; 1998.

Fig. 1.
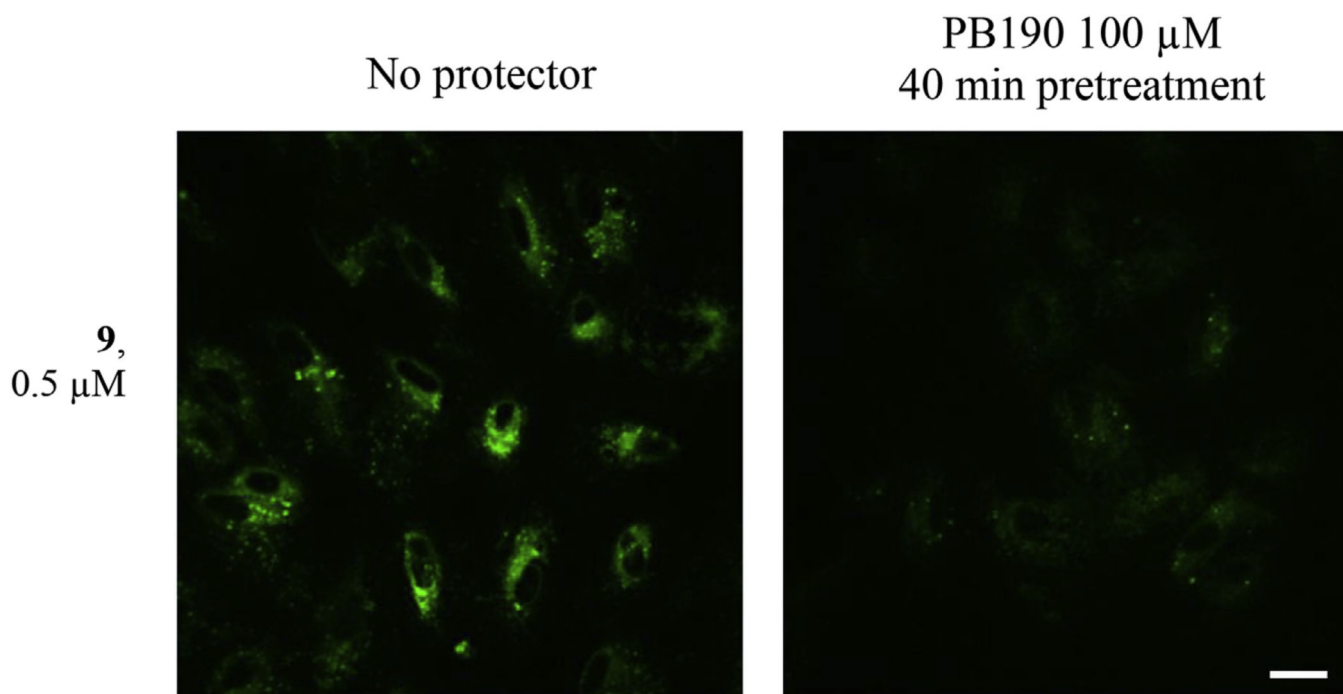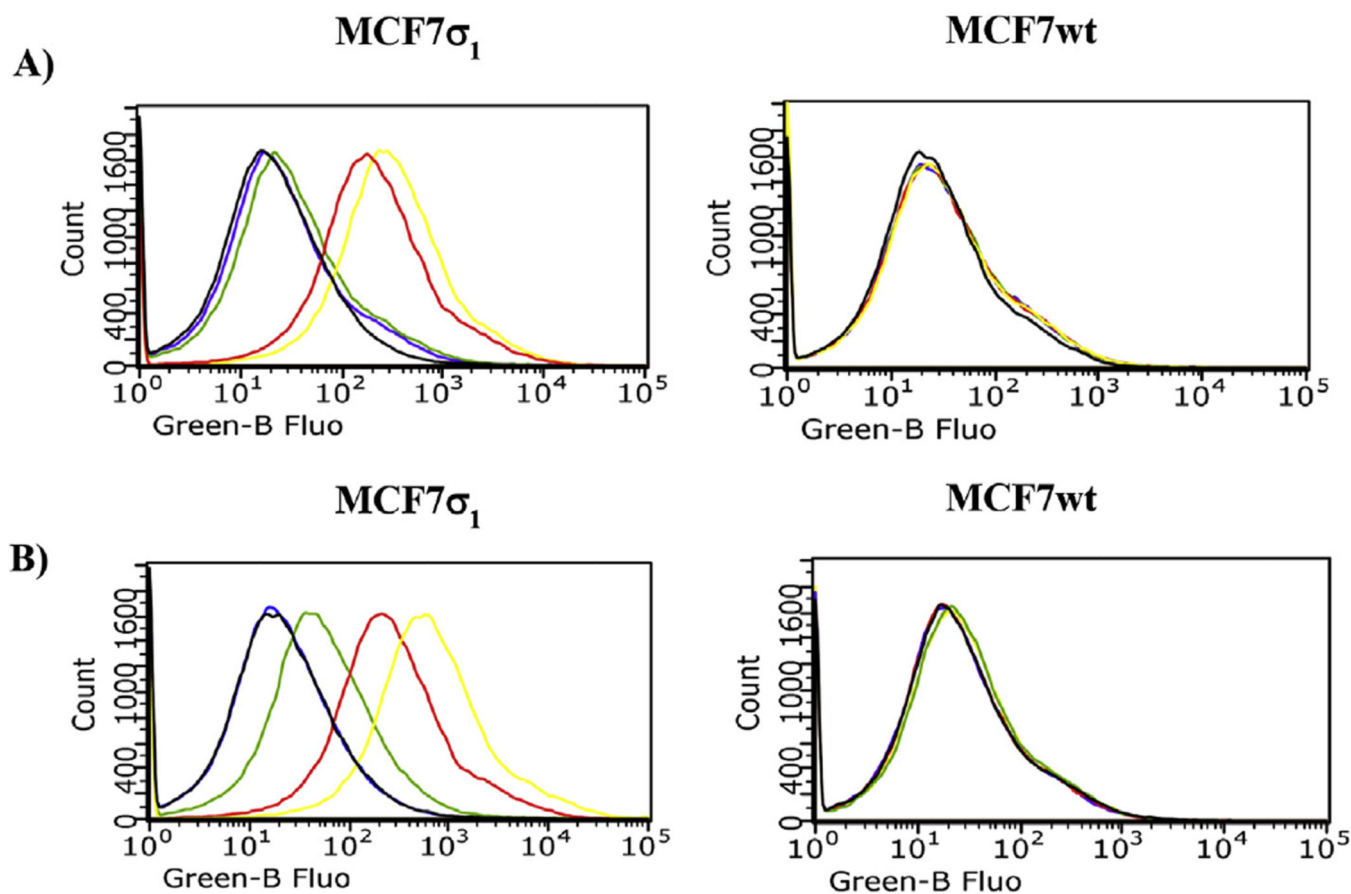σ₁ Receptor lead compounds exploited for the development of σ₁ fluorescent ligands.

Fig. 2. Labeling of ARPE19 Cells with compound 9
Signal is localized to intracellular membranes. Lower intensity of labeling is detected when cells were prelabeled with PB190 100 μM. Scale bar = 20 μm.

Fig. 3.
Flow Cytometry analysis (cell associated fluorescence *vs* cell count) of MCF7σ_1 and MCF7wt, exposed to compound **5** or **6** and treated with compound **10** (10 μM) to mask σ_2 receptors, or (+)-pentazocine (10 μM) to mask σ_1 receptors, or both **10** (10 μM) with (+)-pentazocine (10 μM). A) Displacement of **5** (100 nM, yellow curve): black curve: control; red curve: 10 μM **10**; green curve: 10 μM (+)-pentazo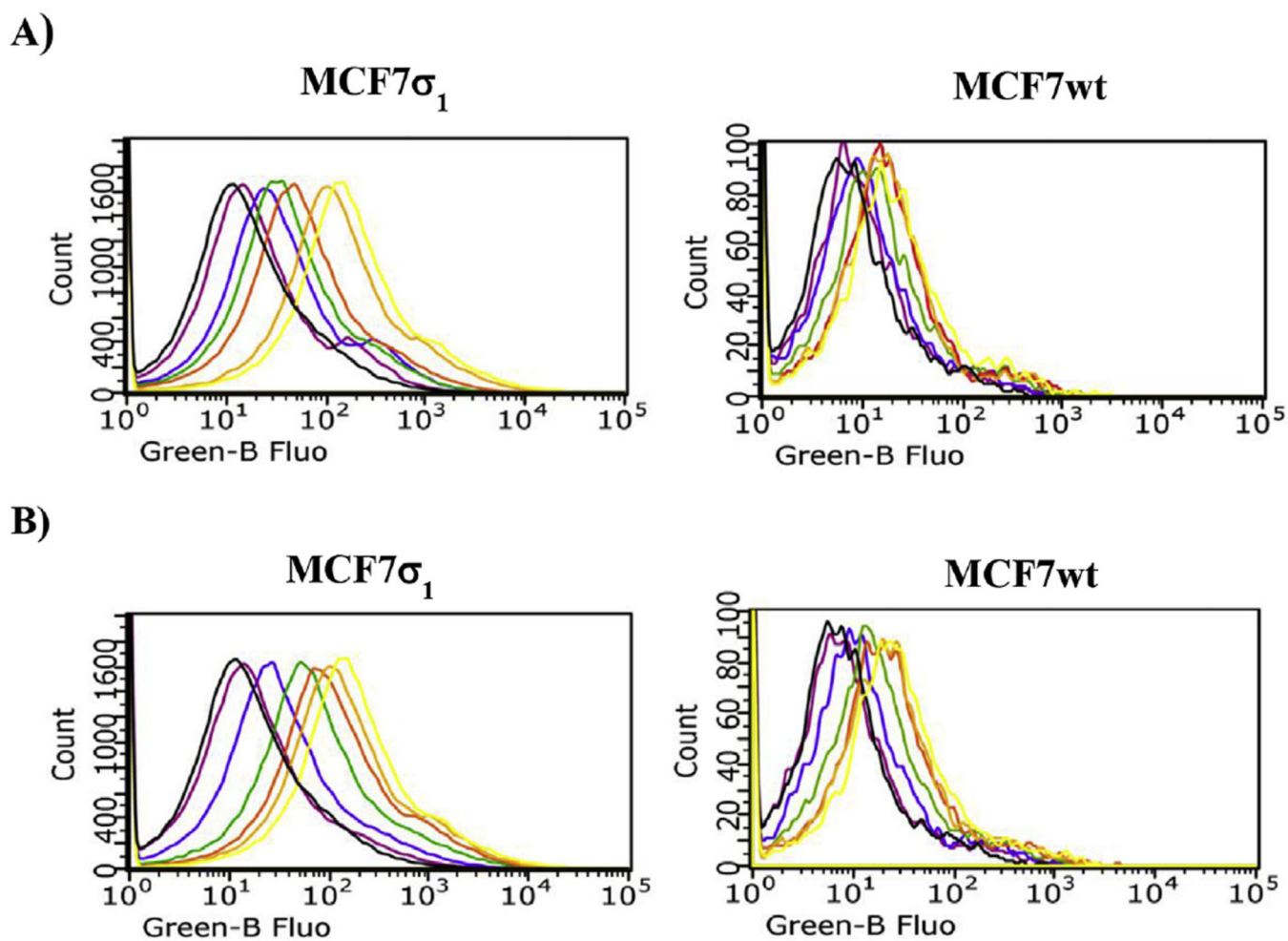cine; violet curve: 10 μM **10** with (+)-pentazocine 10 μM. B) Displacement of **6** (100 nM, yellow curve): black curve: control; red curve: 10 μM **10**; green curve: 10 μM (+)-pentazocine; violet curve: 10 μM **10** with (+)-pentazocine 10 μM.

Fig. 4.
Flow Cytometry analysis (cell associated fluorescence vs cell count) of MCF7σ_1 and MCF7wt, exposed to **5** and treated with **10** (10 μM) to mask σ_2 receptors. A) Displacement of **5** (100 nM, yellow curve) with increasing concentrations of PB190: black curve: control; orange curve: 1 nM PB190; red curve: 10 nM PB190; green curve: 100 nM PB190; blue curve: 1 μM PB190; violet curve: 10 μM PB190. B) Displacement of **5** (100 nM, yellow curve) with increasing concentrations of PB212: black curve: control; orange curve: 1 nM PB212; red curve: 10 nM PB212; green curve: 100 nM PB212; blue curve: 1 μM PB212; violet curve: 10 μM PB212.
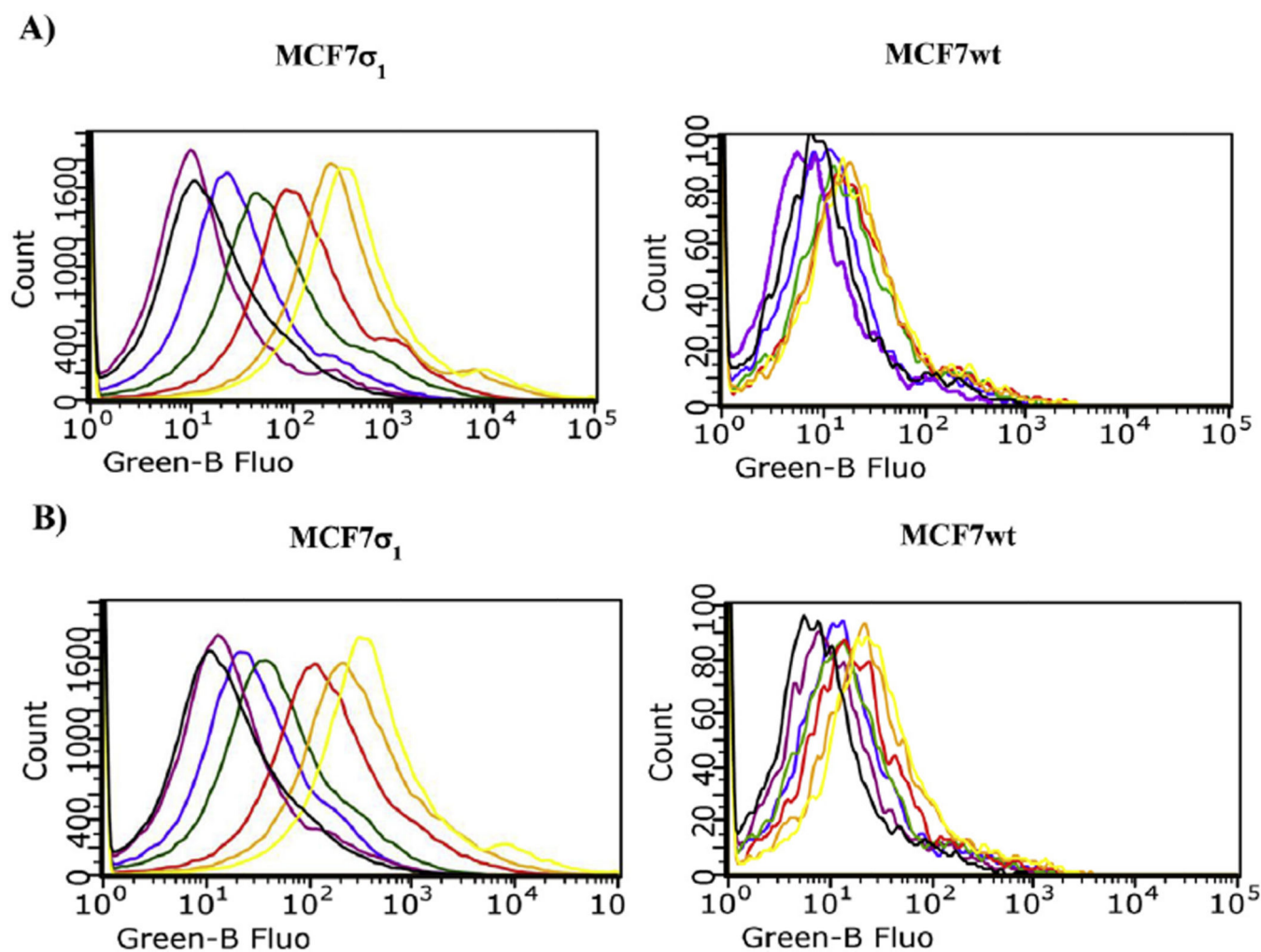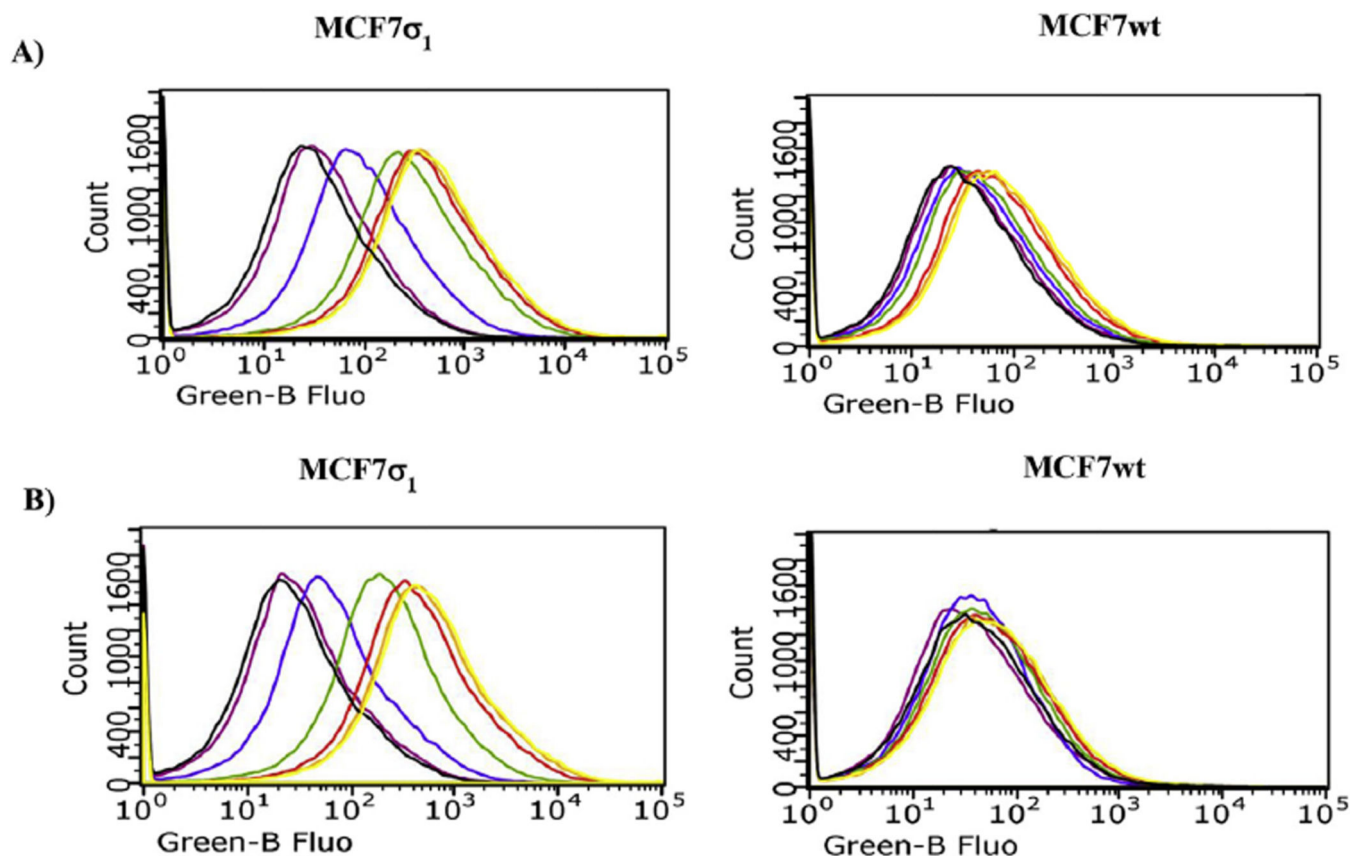
Fig. 5.

Flow cytometry analysis (cell associated fluorescence *vs* cell count) of MCF7σ₁ and MCF7wt, exposed to **6** and treated with **10** (10 μM) to mask σ₂ receptors. A) Displacement of **6** (100 nM, yellow curve) with increasing concentrations of PB190: black curve: control; orange curve: 1 nM PB190; red curve: 10 nM PB190; green curve: 100 nM PB190; blue curve: 1 μM PB190; violet curve: 10 μM PB190. B) Displacement of **6** (100 nM, yellow curve) with increasing concentrations of PB212: black curve: control; orange curve: 1 nM PB212; red curve: 10 nM PB212; green curve: 100 nM PB212; blue curve: 1 μM PB212; violet curve: 10 μM PB212.

Fig. 6.
Flow cytometry analysis (cell associated fluorescence vs cell count) of MCF7σ_1 and
MCF7wt, exposed to **5** or **6** and treated with **10** (10 μM) to mask σ_2 receptors. A)
Displacement of **5** (100 nM, yellow curve) with increasing concentrations of (+)-
pentazocine: black curve: control; orange curve: 1 nM (+)-pentazocine; red curve: 10 nM
(+)-pentazocine; green curve: 100 nM (+)-pentazocine; blue curve: 1 μM (+)-pentazocine;
violet curve: 10 μM (+)-pentazocine. B) Displacement of **6** (100 nM, yellow curve) with
increasing concentrations of (+)-pentazocine: black curve: control; orange curve: 1 nM (+)-
pentazocine; red curve: 10 nM (+)-pentazocine; green curve: 100 nM (+)-pentazocine; blue
curve: 1 μM (+)-pentazocine; violet curve: 10 μM (+)-pentazocine.
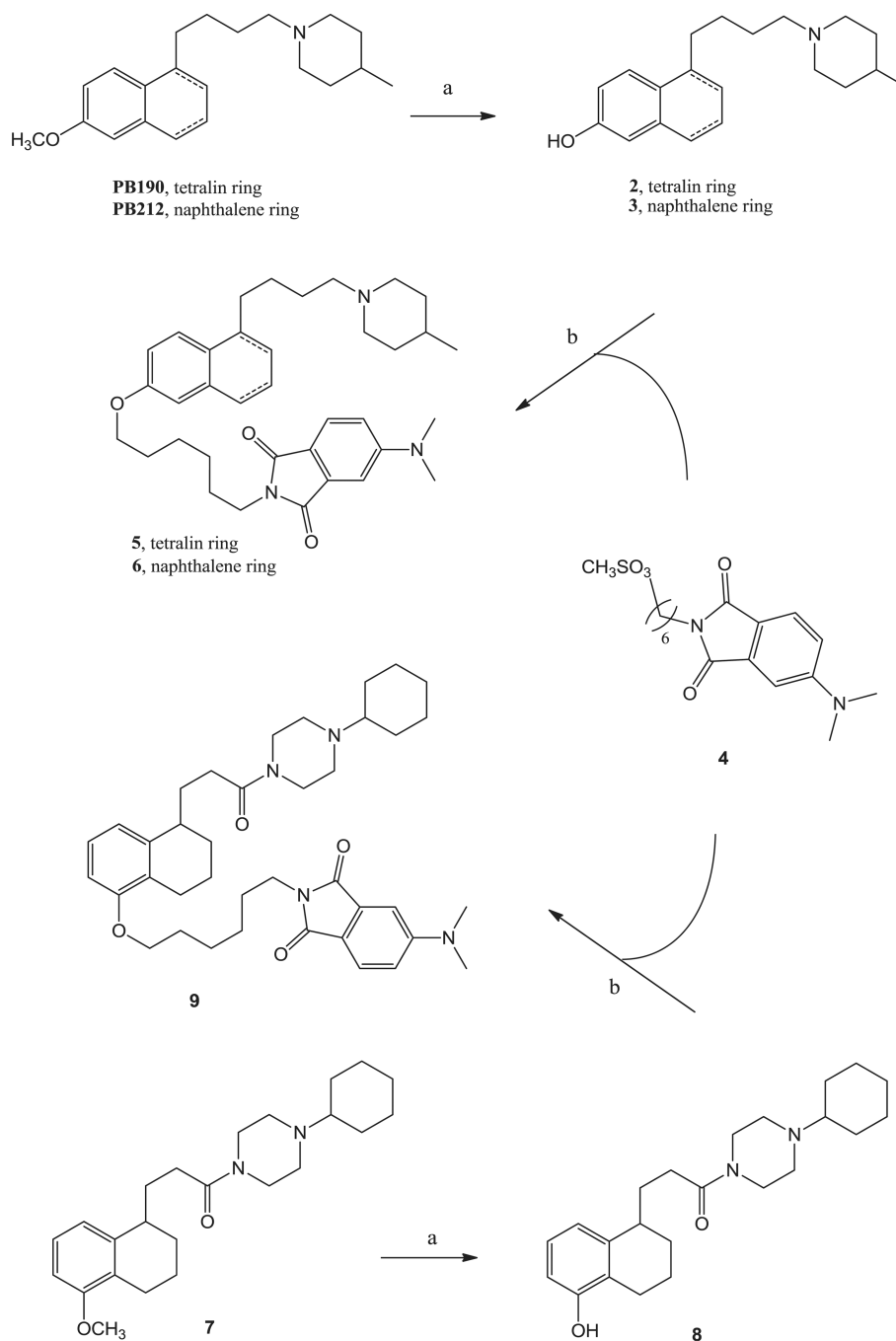
Scheme 1.
Reagents and Conditions: (a) BBr$_3$, CH$_2$Cl$_2$, from −78 °C to room temperature, overnight; (b) K$_2$CO$_3$, DMF, 150 °C, overnight.

Table 1

σ Receptor affinities of final and lead-compounds and fluorescence properties.

Compound	K_i nM ± SEM (nM)^a		λex nm^b	λem nm^b	QY EtOH^c	QY CHCl$_3$^{c}
	σ_1	σ_2				
PB190^d	1.01 ± 0.41	48.7 ± 9.2				
PB212^d	0.03 ± 0.013	17.9 ± 5.3				
1^e	0.11 ± 0.01	179 ± 56				
5	3.61 ± 0.4	48.3 ± 6.0	390	510	0.02	0.5
6	5.20 ± 0.17	45.6 ± 4.6	390	520	0.02	0.4
9	13.1 ± 5.02	38.4 ± 10.9	390	520	0.02	0.4
DTG		35.4 ± 5.8				
(+)-Pentazocine	4.52 ± 0.7					

^{a}Values are the means of n   3 separate experiments, in duplicate.

^{b}Fluorescence properties of compounds were evaluated on compound as free base in EtOH solutions.

^{c}QY was evaluated as in [20].

^{d}Data from Ref. [22].

^{e}Data from Ref. [27].

Table 2

σ$_1$ Receptor affinities of reference σ$_1$ receptor ligands by flow-cytometry with novel σ$_1$ fluorescent ligands.

	σ$_1$; IC$_{50}$ nM ± SEM[a]	
compound	5[b]	6[b]
PB190[c]	11.3 ± 2.4	12.1 ± 1.4
PB212[c]	15.5 ± 2.3	10.6 ± 1.2
(+)-Pentazocine[d]	8.24 ± 1.2	7.59 ± 0.8

[a]Values are the means of n 2 separate experiments, in duplicate.

[b]IC$_{50}$ values from binding curves obtained by dose dependent displacement of **5** (100 nM) or **6** (100 nM) by σ$_1$ reference compounds (PB190, PB212 and (+)-pentazocine) in MCF7σ$_1$ cells by flow cytometry.

[c]Data from 75 min incubation time.

[d]Data from 45 min incubation time. The experiments were performed in the presence of the σ$_2$ masking agent **10** (10 μM).